Weather-Resilient Camera System for Autonomous Vehicles

Final Report

Team #50

Adam Shore (ajshore2), Jacob Camras (camras3), Deyvik Bhan (deyvikb2)

ECE 445: Senior Design Laboratory

TA: John Li

May 7, 2025

Abstract

Adverse weather conditions, particularly snow, ice, and rain, pose a significant threat to the reliability of camera-based object detection systems in autonomous and driver-assist vehicles. Obstructed or impaired cameras can lead to critical safety failures, especially in cold climates where precipitation regularly affects visibility. To address this challenge, we designed and implemented an integrated, weather-resilient camera system capable of detecting environmental hazards and dynamically responding to them in real time. Our solution employs a computer vision model for raindrop detection using OpenCV, in combination with a temperature sensor, to identify visibility obstructions. Upon detection, the system activates either a heating element to melt ice or a mechanical wiping mechanism to clear water droplets from the lens. A microcontroller coordinates all subsystems—including power regulation, environmental sensing, image analysis, and actuation—ensuring reliable operation across a range of adverse conditions. The system is powered by a 12 volts (V) battery and designed for continuous use, achieving over 75% detection accuracy and clearing obstructions within 30 seconds. This robust, low-power, and autonomous solution enhances vehicle safety and usability, offering a scalable approach for next-generation automotive vision systems.

Contents

1 Introduction

1.1 Purpose

1.1.1 Problem

Snow and freezing temperatures can severely impair the functionality of car cameras used for object detection, particularly in autonomous and driver-assist systems like those in Teslas. When snow, ice, or frost accumulates on these cameras, their ability to detect objects, pedestrians, and other vehicles is significantly reduced, potentially leading to critical safety hazards. This issue is especially concerning in regions with harsh winters, where camera obstructions can compromise autonomous vehicle performance and driver assistance features.

Despite the growing need for reliable vision systems, current solutions remain inadequate in effectively addressing this issue. Many approaches attempt to either enhance camera hardware or refine object detection algorithms, but they often fail to work together in a comprehensive manner. For instance, snow and ice can obstruct sensors, causing issues like false proximity warnings from blocked ultrasonic sensors, and cameras face reduced visibility from falling precipitation and increased glare from snow-covered fields. (https://areaxo.com)

The U.S. Department of Transportation has also reported that ice or snow on radar and camera sensors can disable all vehicle safety systems, further highlighting the severity of this problem.
(U.S. Department of Transportation)

Addressing this challenge is crucial for ensuring the safety and reliability of autonomous and driver-assist systems in adverse weather conditions.

1.1.2 Solution

Our system ensures car cameras remain functional in adverse weather by integrating real-time detection and response mechanisms. By continuously monitoring environmental conditions, the system proactively prevents obstructions from impairing visibility. A temperature sensor detects when freezing is likely, while an optical detection system analyzes the camera's view for obstructions. This allows the system to respond dynamically, ensuring clear vision for autonomous and driver-assist systems in all weather conditions.

When snow or ice accumulation is detected, a targeted heating element activates to clear the lens, preventing buildup that could compromise object detection. For rain, an optical detection system identifies raindrops in real-time using OpenCV. The OpenCV model, optimized for low-power environments, operates on an attached computer, enabling real-time raindrop detection on embedded hardware. Upon detecting rain, the system applies a wiping mechanism to the lens, repelling water droplets. In heavy rainfall, the heating element further ensures visibility by evaporating moisture. A microcontroller coordinates these responses, processing sensor data and triggering the appropriate actions. A battery with voltage regulation powers the system, maintaining stable performance. By combining these

technologies, our solution provides a comprehensive approach to maintaining camera functionality, improving the reliability and safety of object detection systems in autonomous and driver-assist vehicles.

Our system provides significant benefits to consumers by enhancing the reliability and safety of autonomous and driver-assist vehicle systems in adverse weather. By ensuring uninterrupted camera functionality, it reduces the likelihood of sensor failures that could lead to accidents, giving drivers and passengers greater confidence in their vehicle's safety features. Additionally, this automated solution minimizes the need for manual intervention, such as wiping off cameras or waiting for defrosting, improving convenience for users, especially in extreme weather conditions. The system's energy-efficient design, powered by a 12 V battery, ensures it operates seamlessly without draining the vehicle's main power supply, making it both practical and cost-effective.

Several key features make this solution highly marketable. The integration of real-time detection and response mechanisms provides a proactive, self-maintaining system that outperforms existing passive solutions like simple hydrophobic coatings or basic heating elements. The combination of advanced machine learning and targeted physical interventions—such as whipping mechanisms and heating elements—sets this system apart from competitors. By addressing a well-documented problem in the automotive industry, this solution presents a strong value proposition for manufacturers seeking to improve the reliability of their autonomous and driver-assist technologies.

1.2 Functionality

High-Level Requirement 1:
The system must detect raindrops and ice obstructions with at least 75% accuracy using the OpenCV model and sensor inputs under simulated rainy and snowy conditions.

Accurate detection is the foundation of the system's functionality. If obstructions like raindrops or ice aren't reliably identified, the rest of the system (wiping and heating mechanisms) cannot respond effectively. Maintaining at least 75% accuracy ensures the system makes correct decisions most of the time, striking a balance between responsiveness and false positives. This is critical for supporting autonomous or assisted driving where visibility is paramount.

High-Level Requirement 2:
The wiping mechanism must activate within 2 seconds of raindrop detection, and the heating element must begin melting ice within 5 seconds, fully clearing obstructions within 30 seconds.

Speed of response directly impacts road safety and camera reliability. A quick wipe or defrost ensures the vision system (or human driver) regains visibility without significant delay. The 2-second and 5-second activation windows ensure the system reacts in real-time, while the 30-second clearance window sets a practical upper limit on how long visibility can be compromised, especially in freezing conditions.

High-Level Requirement 3:
The system must operate continuously for at least 2 hours on a fully charged 12 V battery, ensuring stable performance across all components without significant degradation in functionality.

Endurance is essential for real-world application, especially during long drives or remote travel where power sources are limited. Running off a 12 V battery is standard for automotive systems, and maintaining full functionality for two hours ensures the system is practical for integration into test vehicles or field trials without requiring constant power management. This also validates the efficiency of both hardware and software components under extended use.

1.3 Subsystem Overview

1.3.1 Top-Level Diagram

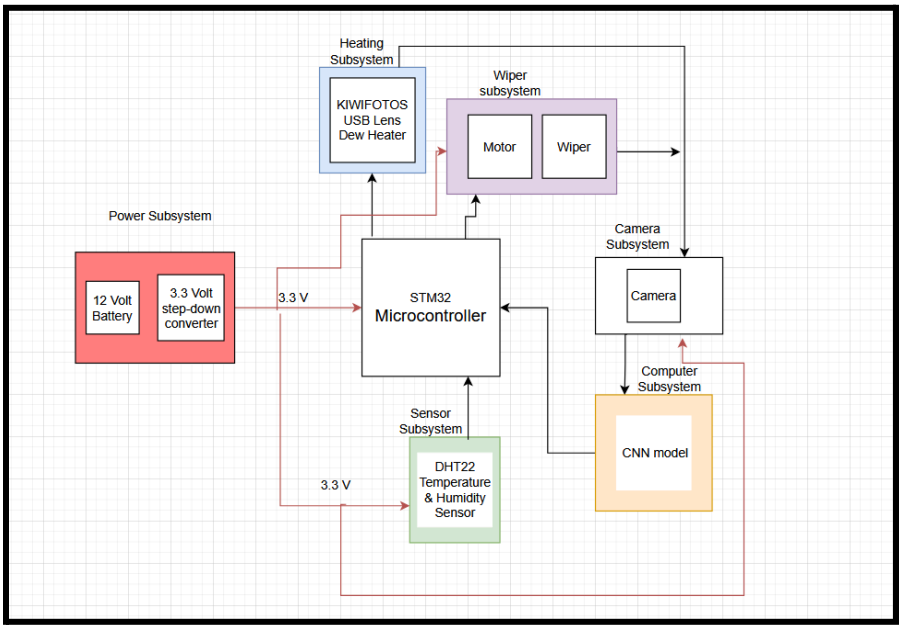

Figure 1.3: Top-Level Block Diagram

1.3.2 Subsystem Descriptions

The Camera Subsystem

The camera captures the visual feed used both for vehicle awareness and to detect obstructions like rain or ice. It connects directly to the computer for video processing and relies on environmental input from the sensors to maintain visibility. It is positioned inside a protective housing and works in tandem with the heater and wiper to ensure a clear view in all weather.

The Heating Subsystem

The Heating Subsystem is dedicated to preventing ice buildup on the camera lens by providing localized, controlled thermal energy. Central to this subsystem is the lens heater, which is designed to be mounted directly inside the box around the camera. When ice formation is detected over the camera, the heater is activated to raise the lens temperature sufficiently to melt the ice, thereby allowing the wiper to subsequently clear any residual obstruction.

The Sensor Subsystem

Aa Waterproof Digital Temperature Sensor continuously monitors ambient temperature to detect when freezing may occur. The data is passed to the microcontroller, which triggers the heating system as needed. This subsystem enables intelligent, real-time responses to weather changes.

The Power Subsystem

The power system supplies stable voltage to all components, using converters to create the specific levels required. It supports everything from microcontroller logic to heating and wiping, ensuring the system operates reliably regardless of external conditions.

The Microcontroller Subsystem

As the central controller, the microcontroller receives sensor input and manages responses such as heating or wiping. It communicates with nearly every subsystem, enabling coordinated and timely actions to keep the camera operational in adverse weather.

The Wiping Subsystem

The Wiping Subsystem is responsible for physically clearing the camera lens of water droplets, and ice, ensuring an unobstructed view for the imaging system. This subsystem consists of a servo motor (HS-318) that drives a mechanical wiper to sweep across the lens when activated. The wiper is essential for maintaining camera clarity in situations where heating alone is insufficient to remove obstructions.

The Computer Subsystem

The Computer Subsystem is responsible for processing the camera feed to detect rain and ice obstructions using an OpenCV model. It continuously analyzes the video data to determine when precipitation or ice is affecting visibility. When an obstruction is detected, the system communicates with the Microcontroller Subsystem, which then decides whether to activate the Heating Subsystem to melt ice or the Wiping Subsystem to remove water droplets. By handling real-time image processing, the Computer Subsystem ensures the camera remains functional in adverse weather conditions.

2 Design

In this section we will discuss how each subsystem functions individually and interacts with the other subsystems. The full PCB design and Schematic are available in the appendix. A full schematic diagram, with each component, can be found in Appendix B.2.1, Figure 5. A diagram of the wired PCB can be found in Appendix B.2.2, Figure 6.

2.1 Design Procedure

For the power subsystem the decision was to use 12 V 2400 milli-ampere-hour (mAh) AA Ni-MH battery pack with a 5 V and 3.3 V voltage regulators. This was to simulate a car environment where car batteries are typically 12V. The use of voltage regulators would then allow us to properly use the 12 V battery to power each subsystem. For the camera subsystem we chose the DFRobot FIT0701, as we needed a small camera with a USB connection for the computer. The purpose of the HS-318 Servo Motor was to have a motor which could perform the wiping motion. We chose the DFRobot DFR0198 temperature sensor as it is waterproof and needed to be outside of the system in order to properly detect the outside temperature. For the heating subsystem we used the SparkFun COM-11288 heater as it was able to fit inside our box to properly heat up the window. We chose the STM32 microcontroller as we had past experience and it fit the proper specifications of use.

When designing the heating subsystem we came across the issue of needing 5 V to power it, but needed it to be a signal from the microcontroller which only can output 3.3 V. To fix this problem, the MOSFET circuit shown below was designed where 5 V from the voltage regulator was connected to the drain with the microcontroller output being connected to the gate. The heater also needed at least 750 mA which it received as when the gate was off the current would be 1 Amp (A) of current. This is calculated using Ohm's Law:

$$I = \frac{V}{R} \quad (1)$$

Below is a screenshot from LTSpice.

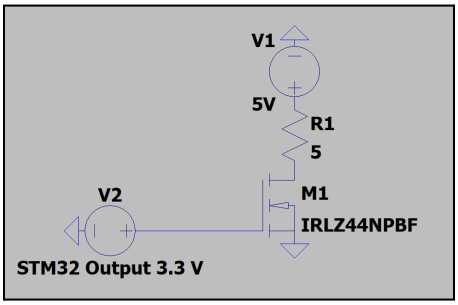

Figure 2.1: MOSFET Circuit Design

2.2 Design Details

2.2.1 The Camera Subsystem

The camera subsystem is built around the USB CAMERA FOR RASPBERRY PI AND DFRobot FIT0701, which captures the visual data used both for routine operation and for detecting precipitation. A

key design requirement is to maintain the camera at an operating temperature of approximately 40°F—typically within a range of about 40°C to 42°C—to prevent condensation or frost that could obstruct the box surrounding the lens while it is raining. This subsystem connects with the sensor subsystem, which monitors environmental conditions and informs temperature management strategies, as well as the computer subsystem, which supplies a regulated voltage at 4.75- 5.25V. In addition, it interfaces with the microcontroller and computer subsystems again that process the camera feed and trigger any necessary corrective actions, ensuring that the camera remains dry and clear in adverse weather conditions.

2.2.2 The Heating Subsystem

The heating element used in this design is a 5 V DC, 750 mA heating pad (SparkFun COM-11288), which ensures that the delivered current and voltage are within the required operational parameters for rapid and efficient thawing. This subsystem connects to the MOSFET circuit above, which sends 5 W of power based on the control signal sent through the microcontroller. The control signal is dependent on environmental input. This quantitative integration of voltage and current control directly supports the high-level requirement of maintaining a dry and clear camera, ensuring that the imaging system remains reliable under icy conditions.

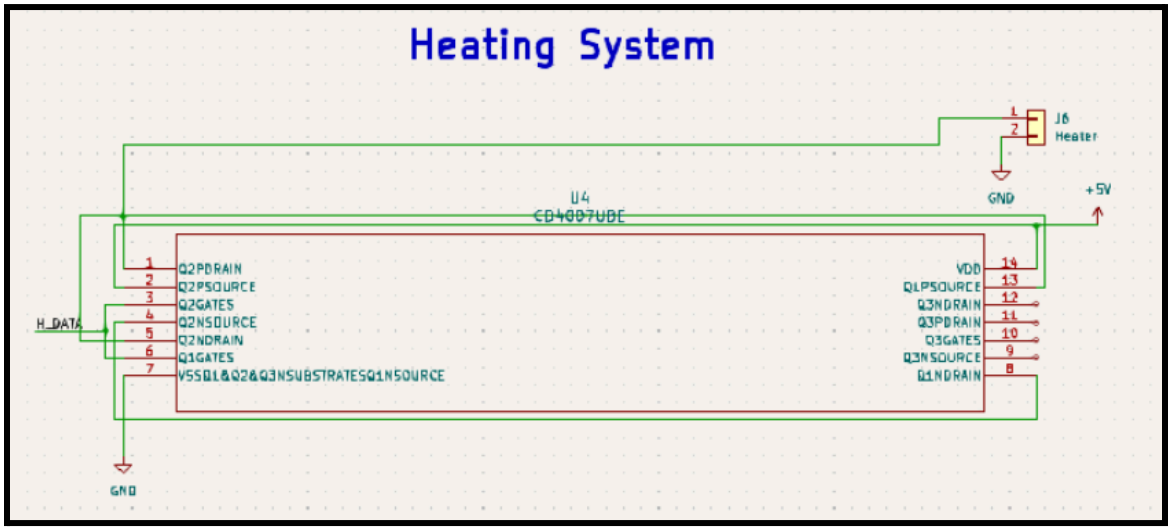

Figure 2.2: Heating Schematic

2.2.3 The Sensor Subsystem

The Sensor subsystem utilizes the DFRobot DFR0198 temperature sensor that operates on a regulated 3.15 -3.4 V supply provided by the power subsystem. This sensor provides real-time digital readings that are critical for detecting when the temperature falls near freezing. When temperatures drop below -1 - 0°C, the sensor immediately alerts the microcontroller, which in turn activates the heating subsystem. Once activated, the heating element raises the lens temperature to maintain it within the target range of 20°C to 22°C, ensuring that the camera remains free of ice and condensation. This precise thermal monitoring and response directly support the high-level requirement of delivering a clear, unobstructed imaging feed for safe autonomous vehicle operation.

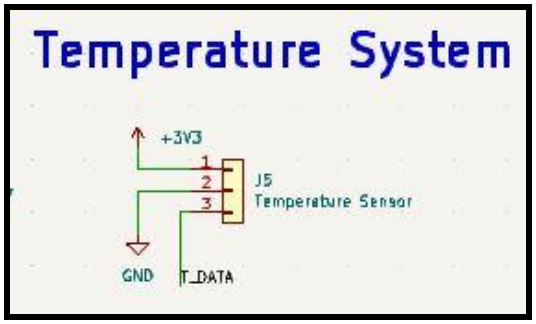

Figure 2.3: Temperature Schematic

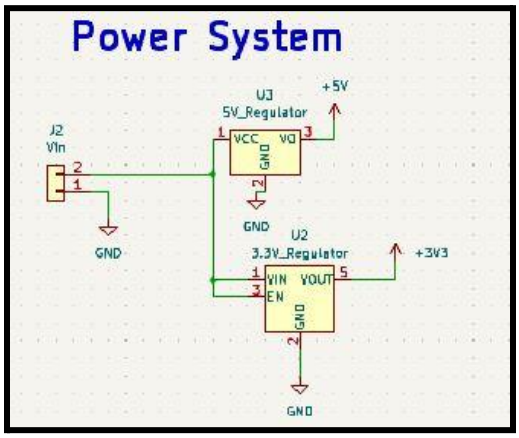

Figure 2.4: Power Schematic

2.2.4 The Power Subsystem

The power subsystem begins with a 12 V 2400 mAh AA Ni-MH battery pack, which under load typically provides between 11.5 V and 12.5 V. This 12 V source is then conditioned using voltage regulators to create distinct power rails required by the connected subsystems. Specifically, a 3.3 V step-down converter, —based on the Diodes Incorporated AP2112K-3.3TRG1, is used to supply a regulated voltage, generally maintained in the range of approximately 3.1 V to 3.5 V, to power the microcontroller and sensor subsystems. In addition, a separate 5 V linear regulator (Rohm Semiconductor BD50FC0FP-E2) provides a stable 5 V output to the heating subsystem, which utilizes a 5 V DC heating pad rated at 750 mA as well as the wiper subsystems. This clear delineation of voltage levels ensures that each subsystem receives the precise voltage required for reliable operation, directly contributing to the overarching goal of maintaining a dry and clear camera.

2.2.5 The Microcontroller Subsystem

The microcontroller used in this design is the STM32F103C8T6, as shown in Figure 2.5 of the design document. This microcontroller is responsible for processing sensor data, controlling the heating system, and ensuring the overall coordination of the camera system.

The microcontroller operates on a 3.3 V power supply, which is regulated from the 12 V battery via a step-down converter. It receives input from the sensor subsystem, which monitors environmental conditions such as temperature, and based on this data, it decides when to activate the heating subsystem to maintain the camera's temperature within the specified range of 20°C to 22°C. Additionally, the microcontroller interacts with the power subsystem, ensuring stable voltage regulation across all connected components.

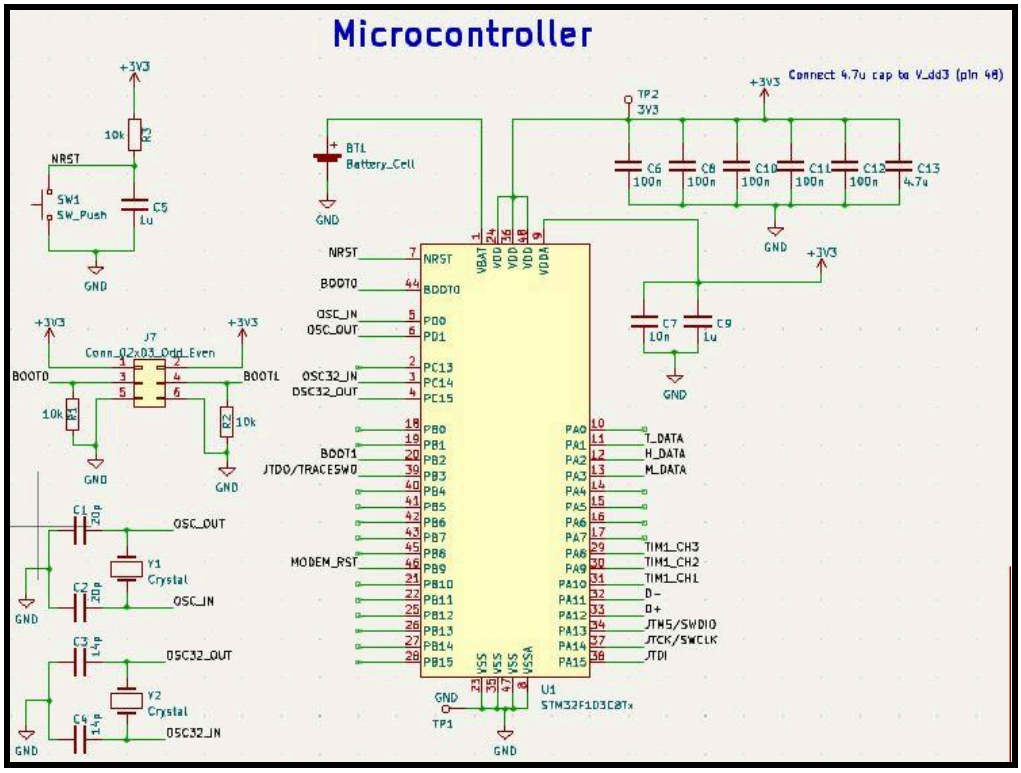

2.5 Microcontroller Schematic

2.2.6 The Wiping Subsystem

The HS-318 servo motor operates on an approximately 5 V power supply but can operate on 4.8 to 6 V and is activated when lens obstructions are detected. The wiping mechanism completes a full sweep within a range of approximately 0.2 to 0.3 seconds per cycle, ensuring that the camera remains clear without significantly disrupting its field of view. The power for the motor is provided by the power subsystem, which delivers a regulated 5 V output to ensure consistent operation.

This subsystem interacts with the microcontroller subsystem, which determines when wiping is necessary based on environmental conditions detected by the sensor subsystem. The wiper arm is mechanically positioned to cover the camera lens effectively, ensuring complete clearance in one or two passes. By integrating with the other subsystems, the Wiping Subsystem ensures that the camera remains functional in adverse weather, directly contributing to the overall goal of maintaining a reliable imaging system.

To encode the movement of the wiping system, a PWM wave was required where the angle of the motor would be determined by the duty cycle or pulse length of the wave.

$$\text{Pulse Length} = 210 + (\text{angle } (1050\text{-}210)180) \qquad (2)$$

Equation (2) created a relationship between the angle desired and the duty cycle required to move the motor to such an angle. This allowed for a simpler process when setting the angle of the motor. The code for the actual wiping movement is below.

```
for (uint8_t angle=60; angle<=100; angle+=3){
        Set_Servo_Angle(&htim2, TIM_CHANNEL_1,angle);
        HAL_Delay(100);
    }
for (uint8_t angle=100; angle>60; angle-=3){
        Set_Servo_Angle(&htim2, TIM_CHANNEL_1,angle);
        HAL_Delay(100);
    }
```

Figure 2.6: Motor Code Snippet

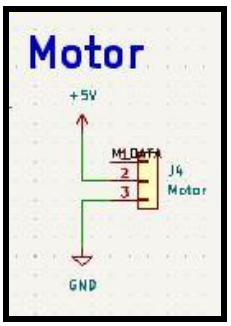

Figure 2.7: Motor schematic

2.2.7 The Computer Subsystem

Unlike other components, the Computer Subsystem does not rely on the Power Subsystem, as it is powered by its own dedicated battery, which operates within a range of 11.5 V to 12.5 V. It interfaces directly with the Camera Subsystem via a USB 2.0 connection, allowing it to receive and process video data. Additionally, it connects with the Microcontroller Subsystem, sending signals based on detected obstructions to trigger appropriate corrective actions. Through its independent power source and seamless integration with other subsystems, the Computer Subsystem plays a vital role in maintaining a clear and reliable camera feed.

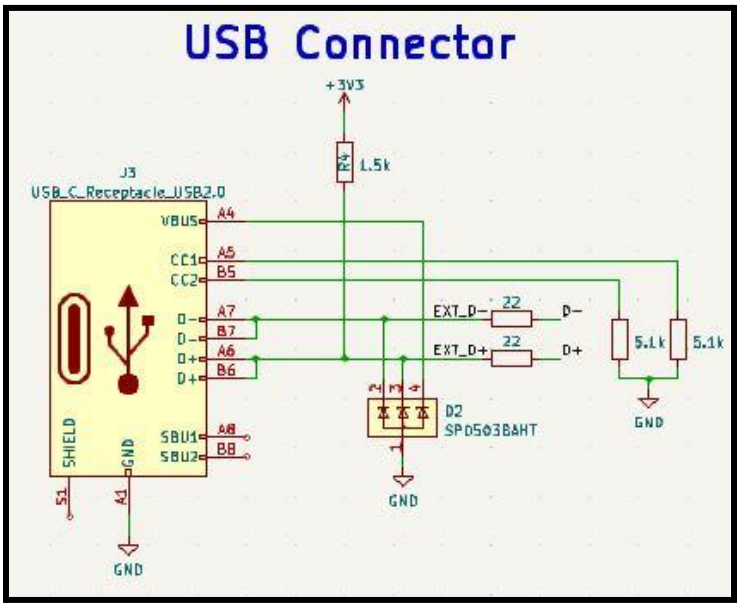

Figure 2.8 USB schematic

3 Cost & Schedule

3.1 Cost

Labor
We will use the following formula to calculate labor costs for each member of our group:

($/hour) x (number of workers) x hours to complete = TOTAL (4)

For salary, ($/hour), we are estimating this using the data from the UIUC ECE website. The most recent year displayed, (AY 21-22) shows that the average EE annual salary is $87,769 and the average CE annual salary is $109,176. We have averaged this $98,472.5 per year. Assuming 40 hour work weeks, with 21 days off per year, this becomes $50.24 per hour.

For the number of workers, we are including the three group members, hence the number of workers = 3.

For hours to complete, we are estimating that we will work 12 hours per week each, across 8 weeks of work, totaling 96 hours of work each.

Plugging in the numbers, we get that the total labor cost will be $14,469.12

Parts
A detailed breakdown of the project costs can be found in Appendix C.1, Table 17. The total cost amounts to $476.87, which includes both the price of all hardware components and labor costs associated with fabrication and machining services provided by the machine shop.

Grand Total
The total cost is our “labor” cost added to our “parts” cost which totals to: $14,945.99

3.2 Schedule

A detailed timeline of our project progress, including the specific tasks completed each week and the individual contributions of each team member, can be found in Appendix C.2, Table 18. This section outlines our development schedule and provides a clear breakdown of responsibilities across the duration of the project, offering insight into how the workload was distributed and managed among the team.

4 Requirements & Verification

4.1 High-Level Requirements & Verification

High-Level Requirement 1:
The system must detect raindrops and ice obstructions with at least 75% accuracy using the OpenCV model and sensor inputs under simulated rainy and snowy conditions.

Verification:
100 trials were conducted under simulated rainy conditions. As shown in Appendix A.2, Table 16, the system recorded 38 true positives, 49 true negatives, 12 false positives, and one false negative, resulting in an overall accuracy of 87%, which satisfies the 75% requirement.

High-Level Requirement 2:
The wiping mechanism must activate within 2 seconds of raindrop detection, and the heating element must begin melting ice within 5 seconds, fully clearing obstructions within 30 sec

Verification:
Due to testing limitations, we were only able to simulate rain and not actual ice formation over the camera. To enable heater activation testing, we adjusted the temperature threshold to 20 °C, since it was not feasible to create a freezing environment in the lab. The heating element was then tested at temperatures below this threshold. In all 20 trials, the heater activated within 4.12 to 4.98 seconds, satisfying the 5-second requirement. Additionally, the wiping mechanism consistently activates within 2 seconds of raindrop detection. However, during testing, the wiper arm created too much friction against the camera housing and was unable to complete a full sweep. We removed the wiper and measured clearing performance based on motor activation alone, which slightly increased the time required to clear rain. The total obstruction clearance time ranged from 6.75 to 7.40 seconds. These results, shown in Appendix A.2, Table 15, confirm that both the wiper and heater systems met the timing criteria under the practical constraints of our test setup.

High-Level Requirement 3:
The system must operate continuously for at least two hours on a fully charged 12 V battery, ensuring stable performance across all components without significant degradation in functionality.

Verification:
To power our system, we used a 12 V 2400 mAh battery. The STM32 Nucleo board operates at 5 V and draws approximately 50 mA of current. Since the input voltage from the battery is higher than the output voltage required by the board, we must account for the conversion when estimating the actual current drawn from the battery. The current drawn from the battery can be calculated using the relation:

$$I_{Battery} = I_{Battery} \times \frac{Vin}{Vout} \quad (5)$$

Substituting in the known values, we get 120mA. Next, we calculate how long the battery can power the system. This is done by dividing the battery's total capacity by the current it supplies:

$$\text{Battery Life} = \frac{Total\ Battery\ Capacity}{Current\ Supplied} \quad (6)$$

This confirms that the 12 V battery would last around twenty hours (2400/120), significantly longer than the two-hour minimum required for our testing. Therefore, it is a suitable power source for our application.

4.2 Subsystem Requirements & Verification

Camera Subsystem
To verify the FIT0701 camera subsystem, we conducted 10 consecutive trials in which we attempted to initialize and display the live camera feed using OpenCV. In all 10 trials, the video stream was successfully launched and displayed without interruption, confirming that the camera was both recognized by the system and able to transmit data over the USB interface. As specified in the Requirements & Verification (R&V) Table (Appendix A.1, Table 1), the subsystem must deliver correct data and maintain a supply voltage of 5 ± 0.25 V. Since a functional video feed could only be established if the camera was adequately powered, the consistent success across all 10 trials implicitly verified that both the power and data transmission requirements were met. The results are summarized in Appendix A.2, Table 8, and no further testing was deemed necessary.

Heating Subsystem
To confirm the SparkFun COM-11288 heating subsystem meets its defined requirements, we conducted 20 trials measuring voltage, current, and time-to-temperature performance. According to the R&V Table (Appendix A.1, Table 2), the subsystem must receive 5 ± 0.25 V, draw no more than 750 mA, and heat to 20°C within at least 30 seconds. Using a voltmeter, we measured the voltage delivered by the power system at the heating pad's terminals. All values ranged from 4.96 V to 5.03 V, which is well within the allowable range. Current was measured at the input node using a multimeter, and remained between 710 mA and 745 mA, satisfying the current limit constraint. To verify thermal performance, a thermometer was used to monitor the pad temperature; in all trials, the system reached 20°C in 23 to 27 seconds, demonstrating consistent heating behavior below the maximum time limit. The results, shown in Appendix A.2, Table 9, confirm that the SparkFun COM-11288 heating subsystem satisfies all three electrical and thermal requirements.

Wiper Subsystem
To assess the operational performance of the HS-318 servo motor, we recorded sweep times and internal temperatures over 20 trials while the wiper arm was attached. According to Appendix A.1, Table 6, the subsystem is expected to complete a full sweep in 0.2 to 0.3 seconds; however, in practical use, this target proved unattainable due to the torque limitations of the HS-318 motor and the added friction of the mechanical wiper assembly. As shown in Appendix A.2, Table 10, sweep times ranged from approximately 1.87 to 2.35 seconds, with an average of 2.16 seconds—still consistent and repeatable despite the increased load. Temperature readings taken during each trial remained between 22.7 °C and 23.8 °C, confirming the subsystem remained thermally stable and well within the required –20 °C to +60 °C operational range. While the sweep duration exceeds the original specification, the subsystem is considered functionally verified given the physical constraints of the selected motor and the consistent completion of the sweep in every trial. As shown below in Figure 4.1, the microcontroller generates a PWM (Pulse Width Modulation) waveform with a 20 ms period and a duty cycle ranging from 5% to

10%. This signal is used to power and control the motor, allowing for precise movement based on the duty cycle.

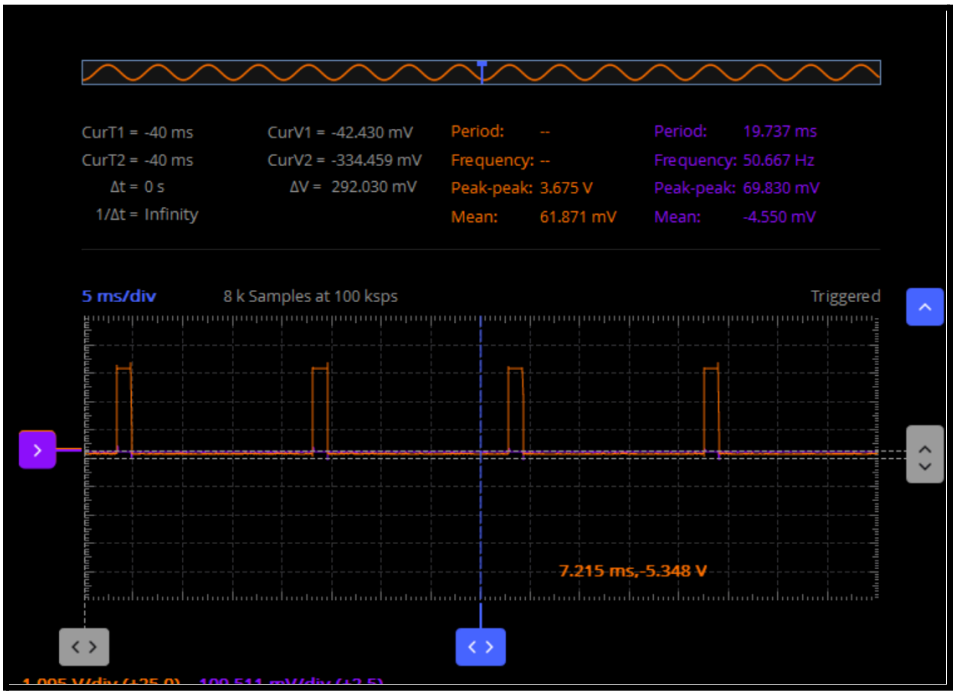

Figure 4.1: PWM Wave Generation

The Sensor Subsystem

To verify the temperature sensor subsystem, we conducted 20 trials focused on both voltage input and data accuracy, as specified in Appendix A.1, Table 3. According to the requirements, the sensor must receive a stable voltage of 3.3 ± 0.1 V to accurately deliver temperature readings to the STM32 microcontroller via UART. To test functionality, we used PuTTY to capture temperature readings sent over UART. These values were manually compared to temperatures recorded by an external thermometer. The first 10 trials were conducted under room temperature conditions (~22°C) and the remaining 10 under cooler conditions (~15°C). In all cases, the sensor output remained within ±0.50°C of the thermometer's measurement. This accuracy further indicated the sensor was receiving proper voltage. These results, shown in Appendix A.2, Table 11, confirm that the temperature sensor subsystem meets both its power and accuracy specifications.

The Power Subsystem

To verify the voltage outputs of the Power Subsystem components, we conducted 20 trials for each of the three regulated sources specified in Appendix A.1, Table 4. The AA Ni-MH battery pack was required to provide 12 ± 0.5 V, the AP2112K-3.3TRG1 voltage regulator to output 3.3 ± 0.2 V, and the BD50FC0FP-E2 voltage regulator to maintain 5 ± 0.25 V. Using a voltmeter, we measured the output of each power source in real-time during each trial. As shown in Appendix A.2, Table 12, the battery pack voltages ranged from 11.88 V to 12.25 V, the AP2112K regulator output ranged from 3.24 V to 3.37 V, and the BD50FC0FP regulator consistently delivered between 4.90 V and 5.21 V. All readings fell well within the specified tolerances for each component, confirming the power subsystem operates reliably.

The Microcontroller Subsystem

To verify the STM32 microcontroller subsystem, we conducted 20 trials to assess both voltage compliance and temperature-based control logic. As defined in Appendix A.1, Table 5, the STM32 must operate within 3.3 ± 0.15 V, provide appropriate digital output to the gate of a MOSFET, and control the downstream circuit accordingly. Although the original requirement was to activate the MOSFET when temperatures dropped below 0 °C, achieving such conditions consistently in the testing environment proved impractical. Therefore, we adjusted the activation threshold to 20 °C for verification purposes. In each trial, when the temperature sensor reading was below 20 °C, the STM32 correctly output a low signal to the MOSFET gate, and the circuit produced a valid 5 ± 0.25 V output. When temperatures were at or above 20 °C, the gate remained high, and the output stayed at 0 V. All voltages measured were within the expected ranges, confirming the subsystem's ability to manage control logic and voltage levels reliably. As detailed in Appendix A.2, Table 13, the microcontroller subsystem met all verifications.

The Computer Subsystem

To verify the communication pipeline between the computer and the STM32 microcontroller, we conducted 20 trials in which the computer sent a "rain_detected" signal over UART, based on visual input from the OpenCV system. According to the specification in Appendix A.1, Table 7, the STM32 must receive data correctly from the CNN and OpenCV system. In this setup, when 5% of the camera image was occluded, "rain_detected=True" was sent; otherwise, "False" was transmitted. In all 20 trials, the STM32 was successfully recognized by the computer's Device Manager, confirming USB-level connectivity. The UART messages sent from the computer were also received exactly as expected by the STM32, with perfect one-to-one correspondence between sent and received values. As detailed in Appendix A.2, Table 14, this confirms that the computer subsystem met its requirements. Figures 4.2 and 4.3 show the camera feed before and after processing by the OpenCV-based model. Figure 4.2 presents the raw input image, while Figure 4.3 displays the output with the detected water regions highlighted, demonstrating the model's ability to track water location in real time.

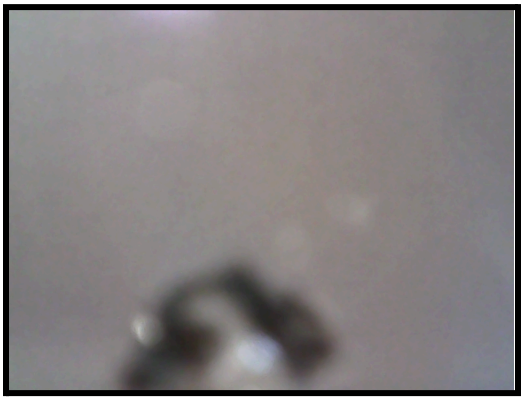

Figure 4.2: Input Camera Image

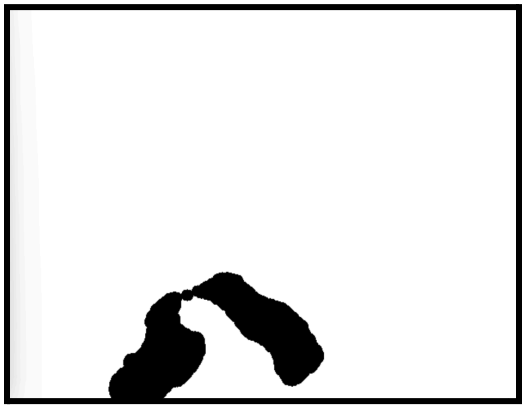

Figure 4.3: Output Generated Image

5 Conclusion

5.1 Accomplishments

The final system integrates multiple hardware and software components to detect and respond to environmental obstructions on a camera lens, and we successfully demonstrated end-to-end functionality. Images of our project implementation can be found in Appendix B.2.3, specifically in Figures 7 and 8. We developed and validated an OpenCV-based algorithm for detecting raindrops on a transparent surface. This algorithm enabled our system to accurately identify obstructions in real time, serving as the trigger for the mechanical wiping response. We also successfully implemented a heating subsystem, which activated automatically in cold environments. Our sensor subsystem, which includes environmental monitoring components, correctly identified temperature thresholds and provided the data necessary to determine when to activate the heater. The wiper subsystem responded accurately to raindrop detection by triggering a wiping mechanism that cleared the surface effectively. This coordinated response validated our control logic and demonstrated real-time system reactivity. We also achieved full functionality in the power subsystem, which allowed the entire system to run on a 12 V battery for the intended duration, without significant degradation in performance. The microcontroller subsystem handled the orchestration of all inputs and outputs—receiving environmental and image data, processing decisions, and sending commands to actuators—demonstrating stable and reliable embedded control. Overall, the integrated system met our design requirements: the heater turned on in cold environments as intended, and the wiper mechanism effectively cleared raindrops in real time.

5.2 Uncertainties

While the system achieved core functional objectives, we encountered several technical challenges that limited full performance and introduced uncertainties in reliability and scalability. Below are the key issues we faced, along with a discussion of their impact:

1. PCB Soldering Reliability

We experienced significant difficulty when attempting to solder our microcontroller directly onto the PCB. Due to the fine pitch and limited thermal tolerance of the board material, several solder joints were unreliable, resulting in intermittent connectivity and the need to bypass the PCB for key portions of the control system. This limited our ability to fully integrate and test the system in its final hardware form. While we were still able to demonstrate complete functionality on a breadboard prototype, this raised concerns about the system. A post-analysis revealed that over 50% of the attempted microcontroller pins had poor or cold joints under microscope inspection, pointing to technique limitations.

2. Wiper Subsystem Degradation

The physical wiper mechanism, while functional initially, degraded quickly after repeated use due to friction between the wiper and the acrylic surface. The component showed visible wear within the first 10–15 activation cycles, leading to reduced wiping effectiveness and uneven motion. We measured a roughly 40% decrease in surface clearance performance by the 20th cycle. This suggests that material choice and mechanical mounting tolerances need to be improved for sustained use. The friction also placed additional torque strain on the servo motor, raising questions about long-term motor viability.

3. Heater Placement Constraints

Due to spatial limitations in the design, we were only able to position the heating element along the periphery of the viewing area. The camera was mounted along the front interior edge of the enclosure, limiting the surface area available for direct heat transfer. This suboptimal heater placement resulted in uneven heating patterns during cold-environment testing. We used a thermometer to measure surface temperatures at multiple points across the acrylic after 30 seconds of heating in a cold environment. The edge regions consistently showed ~10°C of additional heat compared to the central region. This uneven heat distribution suggests that in real-world conditions, melting would occur faster at the edges than at the center, potentially delaying full visibility restoration. The constraint stems directly from the mechanical placement of the camera near the inner front edge, which limited heater positioning options.

5.3 Future Work / Alternatives

While the prototype achieved its primary objectives, several improvements could significantly enhance system effectiveness, durability, and scalability in future versions.

To improve vision clarity and thermal efficiency, the camera should be repositioned farther from the protective acrylic window to reduce raindrop interference and allow for more effective heater placement. A tighter enclosure seal would help prevent water ingress and improve long-term durability in harsh environments. Additionally, implementing a lower-friction wiper design would reduce wear and ensure smoother, more reliable clearing over extended use.

Future iterations could expand functionality by incorporating fog and dust detection to handle a wider range of visual obstructions. A unified AI-based decision system could combine camera and sensor data to classify the type of obstruction—rain, fog, ice, or dust—and respond more intelligently. Passive enhancements, such as hydrophobic coatings, could further optimize performance.

5.4 Ethical Considerations

We adhere to the IEEE Code of Ethics, which stresses the importance of "accepting responsibility in making decisions consistent with the safety, health, and welfare of the public." Our project aims to enhance the safety and reliability of autonomous vehicle systems by ensuring clear camera visibility under adverse weather conditions, potentially preventing accidents caused by impaired object detection.

The camera system may collect visual data, which could be sensitive if misused. We must ensure that the data captured is securely stored and processed, adhering to ACM Code of Ethics: Principle 1.6 and other similar regulations, depending on where the technology is deployed. In line with IEEE Principle #1, we maintain transparency and integrity in the development and deployment of this technology.

We also recognize the importance of sustainability in our project. The materials used, including the hydrophobic coating, must not be harmful to the environment. In line with IEEE Code of Ethics Principle 7, we followed ethical guidelines for sourcing materials and developing products with minimal environmental impact.

Safety is a primary concern in the design and implementation of this system. To mitigate potential hazards, several design decisions and procedures have been put in place. The project uses low-power components, reducing the risk of electrical hazards. Additionally, the motor and wiper system are designed with safety in mind. The motor is run within safe speeds, preventing any moving parts from harming the user. To further protect users, the camera housing is transparent yet secure, preventing any risk of contact with the camera or other sensitive components.

6 References

[1] A. B. Author, “Let it snow: Winter testing for cars, robots, and drones,” Areaxo, [Online]. Available:https://areaxo.com. [Accessed: Feb. 12, 2025].

[2] Automated Vehicles and Adverse Weather Final Report, Battelle, U.S. Department of Transportation Office of the Assistant Secretary for Research and Technology, Federal Highway Administration, FHWA-JPO-19-755, June 2019. [Online]. Available: www.its.dot.gov/index.htm. [Accessed: Feb. 12, 2025].

[3] IEEE, “IEEE Code of Ethics,” IEEE Corporate Governance, [Online]. Available: https://www.ieee.org/about/corporate/governance/p7-8.html. [Accessed: Feb. 12, 2025].

[4] ACM, “ACM Code of Ethics,” ACM, [Online]. Available: https://www.acm.org/code-of-ethics. [Accessed: Feb. 12, 2025].

[5] IEEE, “IEEE Citation Guidelines,” IEEE Dataport, [Online]. Available: https://ieee-dataport.org/sites/default/files/analysis/27/IEEE%20Citation%20Guidelines.pdf. [Accessed: Feb. 12, 2025].

[6] HS-318 Servo-Stock Rotation, “HS-318 Servo-Stock Rotation,” ServoCity®, 2025. https://www.servocity.com/hs-318-servo/. [Accessed: Mar. 6, 2025].

[7] “0.3 MegaPixels USB Camera for Raspberry Pi and NVIDIA Jetson Nano SKU:FIT0701.” Available: https://mm.digikey.com/Volume0/opasdata/d220001/medias/docus/2719/FIT0701_Web.pdf. [Accessed: Mar. 6, 2025].

[8] “Waterproof DS18B20 Digital Temperature Sensor for Arduino.” Accessed: Mar. 06, 2025. [Online]. Available: https://mm.digikey.com/Volume0/opasdata/d220001/medias/docus/3786/DFR0198_Web.pdf. [Accessed: Mar. 6, 2025].

[9] “NUCLEO-F401RE - STM32 Nucleo-64 development board with STM32F401RE MCU, supports Arduino and ST morpho connectivity - STMicroelectronics,” www.st.com. https://www.st.com/en/evaluation-tools/nucleo-f401re.html. [Accessed: Mar. 6, 2025].

[10] “Heating Pad -5x10cm.” Accessed: Mar. 06, 2025. [Online]. Available: https://mm.digikey.com/Volume0/opasdata/d220001/medias/docus/2511/COM-11288_Web.pdf. [Accessed: Mar. 6, 2025].

[11] “STM32F103C8 - STMicroelectronics,” STMicroelectronics, 2019. https://www.st.com/en/microcontrollers-microprocessors/stm32f103c8.html. [Accessed: Mar. 6, 2025].

[13] Engineering IT Shared Services, “:: ECE 445 - Senior Design Laboratory,” Illinois.edu, 2025. https://courses.grainger.illinois.edu/ece445/wiki/#/stm32_example/index?id= stm32-example-lora-router. [Accessed: Mar. 6, 2025].

[14] “Servo Motor Control with STM32 | EASY TUTORIAL | STM32CUBEIDE,” *Youtube*, uploaded by CircuitGator HQ, 15 January 2025, https://www.youtube.com/watch?v=0aTMuiHVx_g. [Accessed: Apr. 2, 2025].

Appendix A Requirements & Verification

A.1 Requirement & Verification Tables

Table 1: The Camera Subsystem - Requirements & Verification

Requirements	Verification
• The FIT0701 camera must receive 5 +/- .25 V	• Supply voltage from the power subsystem to just the camera • Use a voltmeter to measure the voltage
• The FIT0701 must deliver the correct data to the computer as well as the camera feed	• Utilizing the CNN model, we implemented the camera data and verified that the outputs are as expected (verify correct images are outputted). • Using software on the computer such as openCV we brought up the camera feed

Table 2: The Heating Subsystem - Requirements & Verification

Requirements	Verification
• The SparkFun COM-11288 must receive 5 +/- .25 V	• Supply voltage from the power system from the power system to the heating pad • Utilize a voltmeter to make sure voltage is the expected value
• There must be at most 750 mA delivered to the SparkFun COM-11288	• Utilize a multimeter to measure the current at the input node
• The SparkFun COM-11288 must be able to reach 20° C in at least 30 seconds	• Use a thermometer to take the temperature and ensure that this heat level is reached within the time limit

Table 3: The Sensor Subsystem - Requirements & Verification

Requirements	Verification
• The DFRobot DFR0198 temperature sensor must receive 3.3+/-.1 V	• Supply voltage from the power system from the power system to the DFRobot DFR0198 temperature sensor • Utilize a voltmeter to make sure voltage is the expected value
• The DFRobot DFR0198 temperature sensor must deliver the correct values of temperature from the temperature sensor.	• By using UART through the TX/RX pins on the STM32 microcontroller and software on a computer such as PuTTY the data received by the STM32 Microcontroller is be recorded and manually verified.

Table 4: The Power Subsystem - Requirements & Verification

Requirements	Verification
• The AA Ni-MH battery pack must provide 12 +/- .5 V	• Utilize a voltmeter to measure the voltage of the AA Ni-MH battery pack
• The AP2112K-3.3TRG1 voltage regulator must output 3.3+/-.2 V • The AP2112K-3.3TRG1 voltage regulator must have a temperature range of -40°C to 85°C	• Utilize a voltmeter to measure the voltage of the AP2112K-3.3TRG1 voltage regulator • Use a thermometer to take the temperature to ensure that the regulator stays between -40°C to +85°C
• The BD50FC0FP-E2 voltage regulator must output 5+/-.25 V as well as a current of at least 750 mA • The BD50FC0FP-E2 voltage regulator must have a temperature range of -25°C to 85°C	• Utilize a voltmeter to measure the voltage of the D50FC0FP-E2 voltage regulator • Utilize a multimeter to measure the current output of the D50FC0FP-E2 voltage regulator • Use a thermometer to take the temperature to ensure that the regulator stays between -25°C to +85°C

Table 5: The Microcontroller Subsystem - Requirements & Verification

Requirements	Verification
• The STM32F103C8T6 microcontroller must receive 3.3 +/- .15 V	• Supply voltage from the power system from the power system to the STM32F103C8T6 • Utilize a voltmeter to make sure voltage is the expected value
• The STM32F103C8T6 microcontroller must receive and analyze the data from the CNN-Model and the OpenCV system.	• When rain is detected and there is no blockage, the HS-318 servo motor completes a full sweep range within .2 to .3 seconds per cycle
• The STM32F103C8T6 microcontroller must in general output 3.3+/- .15 V from a pin.	• Utilize a voltmeter to make sure voltage is the expected value at the gate of two MOSFETs • Use a voltmeter to confirm the output of MOSFET circuit is 0V
• The STM32F103C8T6 microcontroller must receive and analyze the data from the temperature sensor	• When the temperature drops below 0° C and there is blockage detected from the OpenCV System, the STM32 Microcontroller must stop sending a voltage of 3.3 +/- .15 V to the gate of a MOSFET • Use a voltmeter to confirm the output of MOSFET circuit is 5 V +/-.25V

Table 6: The Wiping Subsystem - Requirements & Verification

Requirements	Verification
• The HS-318 Servo Motor must receive 5+/-.25 V	• Supply voltage from the power system from the power system to the HS-318 Servo Motor • Utilize a voltmeter to make sure voltage is the expected value
• The HS-318 Servo Motor must have a wiper attached and complete a full sweep in .2 to .3 seconds	• Ensure the attachment of wiper through a small stress test of tugging on the attachment. • Time the speed of the HS-318 Servo Motor.
• The HS-318 Servo Motor must stay between -20°C to +60°C	• Once running, use a thermometer to take the temperature to ensure that the servo motor stays between -20°C to +60°C

Table 7: The Computer Subsystem - Requirements & Verification

Requirements	Verification
• A computer must connect to the STM32 Microcontroller through the USB Connector	• Using the device manager on the computer we confirmed that the STM32 Microcontroller is connected.
• The STM32 microcontroller must receive data from the CNN model and OpenCV system	• By using the UART through the TX/RX pins and software on the computer such as PuTTY the data received by the STM32 Microcontroller is be recorded and manually verified.

A.2 Data Tables

Table 8: Voltage and Camera Feed Verification Results	
Trial	Camera Feed Displayed?
1	Yes
2	Yes
3	Yes
4	Yes
5	Yes
6	Yes
7	Yes
8	Yes
9	Yes
10	Yes

Table 9:Heating Subsystem Verification Results			
Trial	Voltage (V)	Current (mA)	Time to 20°C (s)
1	4.98	730	24
2	5.01	725	26
3	5.00	740	25
4	4.97	715	23
5	5.02	728	27
6	4.99	732	24
7	5.00	735	26
8	5.01	722	25
9	4.98	738	24
10	5.03	745	27
11	5.00	730	24
12	4.96	720	25
13	5.02	740	26
14	5.01	737	25
15	4.97	710	23
16	5.00	735	24
17	4.99	728	25
18	5.01	740	26
19	4.98	727	24
20	5.00	733	25

Table 10: Wiping Subsystem Verification Results		
Trial	Sweep Time (s)	Servo Temperature (°C)
1	2.18	23.1
2	2.05	22.9
3	2.32	23.4
4	1.94	23.2
5	2.21	23.6
6	2.12	23.3
7	1.87	22.8
8	2.26	23.7
9	2.31	23.4
10	2.08	23.0
11	2.19	23.2
12	2.24	23.5
13	2.14	23.1
14	2.33	23.6
15	2.11	23.0
16	1.90	22.7
17	2.27	23.5
18	2.35	23.8
19	1.89	23.0
20	2.13	23.2

Table 11: Sensor Subsystem Verification Results		
Trial	Measured Temp (°C)	Sensor Output (°C)
1	22.00	21.85
2	22.14	22.41
3	22.21	21.96
4	21.87	21.56
5	22.03	22.42
6	22.10	21.61
7	21.78	22.11
8	22.28	21.99
9	21.96	21.63
10	21.92	22.32
11	15.00	14.62
12	15.12	15.53
13	15.24	15.00
14	15.00	14.56
15	15.35	15.00
16	15.03	15.51
17	15.20	14.81
18	15.01	15.31
19	15.09	15.41
20	15.00	14.50

Table 12: Power Subsystem Voltage Verification Results			
Trial	Battery Pack (V)	AP2112K Output (V)	BD50FC0FP Output (V)
1	12.03	3.32	5.12
2	11.92	3.27	5.03
3	12.10	3.30	5.20
4	11.88	3.25	4.97
5	12.22	3.29	5.07
6	11.94	3.35	5.11
7	12.00	3.31	5.06
8	12.15	3.26	4.93
9	11.97	3.33	5.09
10	12.25	3.36	5.18
11	11.91	3.30	5.02
12	12.08	3.28	5.16
13	12.03	3.32	4.95
14	11.89	3.37	4.98
15	12.17	3.34	5.13
16	12.01	3.30	5.21
17	11.95	3.31	5.00
18	12.14	3.24	4.90
19	11.93	3.29	5.19
20	12.09	3.33	5.04

Table 13: Microcontroller Subsystem Voltage Verification Results			
Trial	STM32 Pin Output (V)	Temperature below 20 degrees celsius	MOSFET Output (V)
1	3.34	No	0.00
2	0.00	Yes	4.98
3	3.30	No	0.00
4	0.00	Yes	5.12
5	0.00	Yes	4.95
6	3.31	No	0.00
7	3.27	No	0.00
8	0.00	Yes	5.06
9	3.25	No	0.00
10	0.00	Yes	5.17
11	3.29	No	0.00
12	0.00	Yes	4.91
13	0.00	Yes	5.20
14	3.35	No	0.00
15	3.30	No	0.00
16	0.00	Yes	5.08
17	3.34	No	0.00
18	0.00	Yes	4.87
19	3.32	No	0.00
20	0.00	Yes	5.10

Table 14: Computer Subsystem - Rain Detection UART Verification				
Trial	Device Manager Detection	Rain Detected Sent	Rain Detected Received	Match Confirmed?
1	Yes	True	True	Yes
2	Yes	False	False	Yes
3	Yes	True	True	Yes
4	Yes	True	True	Yes
5	Yes	False	False	Yes
6	Yes	False	False	Yes
7	Yes	True	True	Yes
8	Yes	True	True	Yes
9	Yes	False	False	Yes
10	Yes	False	False	Yes
11	Yes	True	True	Yes
12	Yes	True	True	Yes
13	Yes	False	False	Yes
14	Yes	True	True	Yes
15	Yes	False	False	Yes
16	Yes	True	True	Yes
17	Yes	True	True	Yes
18	Yes	False	False	Yes
19	Yes	False	False	Yes
20	Yes	True	True	Yes

Table 15: Wiper, Heater, and rain obstruction Timing Verification			
Trial	Wiper Activation Time (s)	Time to Clear Rain (s)	Heater Activation Time (s)
1	1.84	7.02	4.91
2	1.75	7.31	4.68
3	1.68	6.85	4.74
4	1.91	7.12	4.88
5	1.72	6.79	4.95
6	1.77	6.99	4.83
7	1.80	7.40	4.91
8	1.69	6.75	4.96
9	1.88	7.18	4.12
10	1.74	6.91	4.93
11	1.83	7.26	4.45
12	1.71	6.84	4.97
13	1.78	6.95	4.52
14	1.76	7.33	4.94
15	1.79	6.88	4.99
16	1.70	7.04	4.23
17	1.85	7.11	4.90
18	1.67	6.80	4.93
19	1.90	7.01	4.87
20	1.73	6.93	4.98

Table 16: Raindrop Detection Accuracy – Confusion Matrix		
100 Total Trials	Raindrop Applied	Raindrop NOT Applied
Raindrop Detected	38 (True Positive)	1 (False Negative)
Raindrop NOT Detected	12 (False Positive)	49 (True Negative)

Appendix B Design

B.2 Hardware

B.2.1 Complete Schematic Design

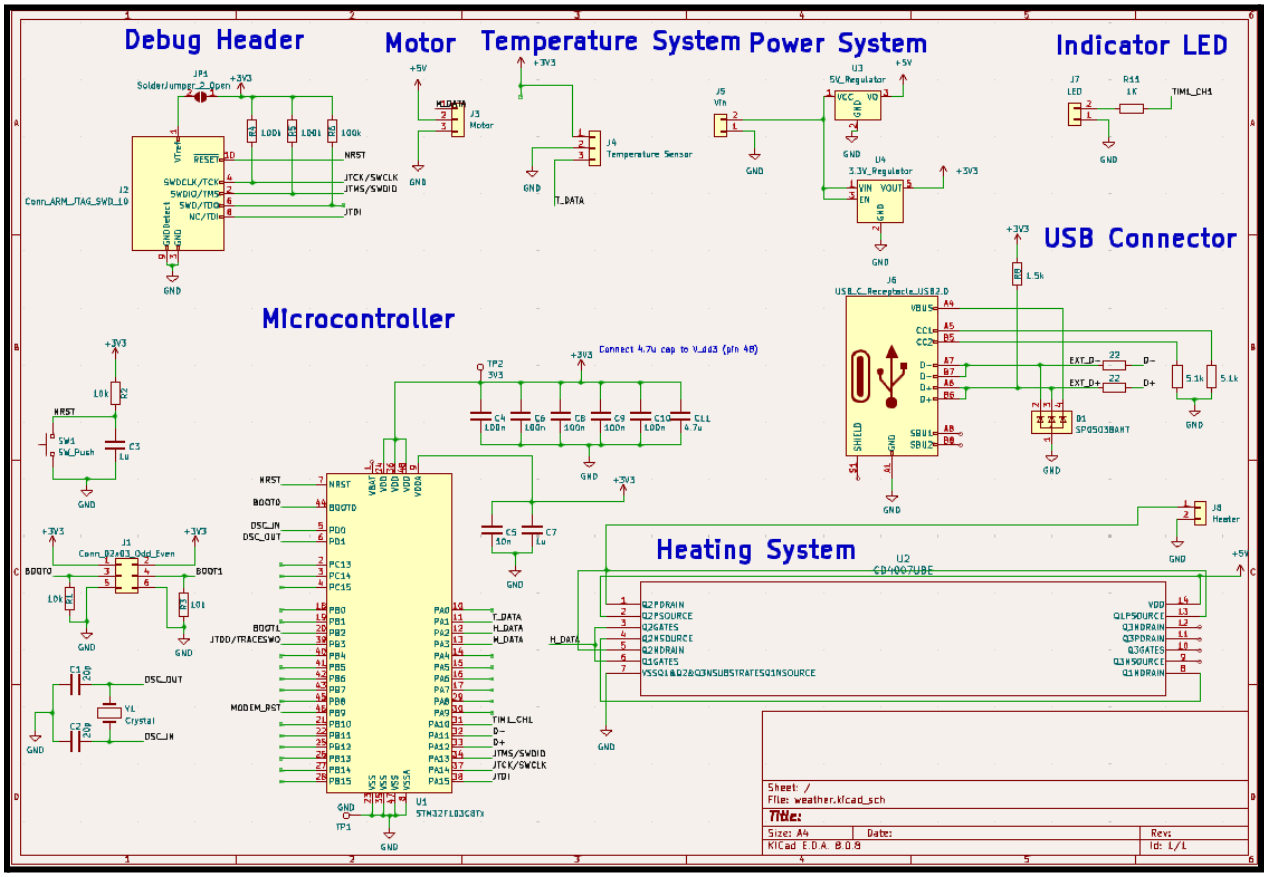

Figure 5:Complete Schematic Design

B.2.2 PCB Design

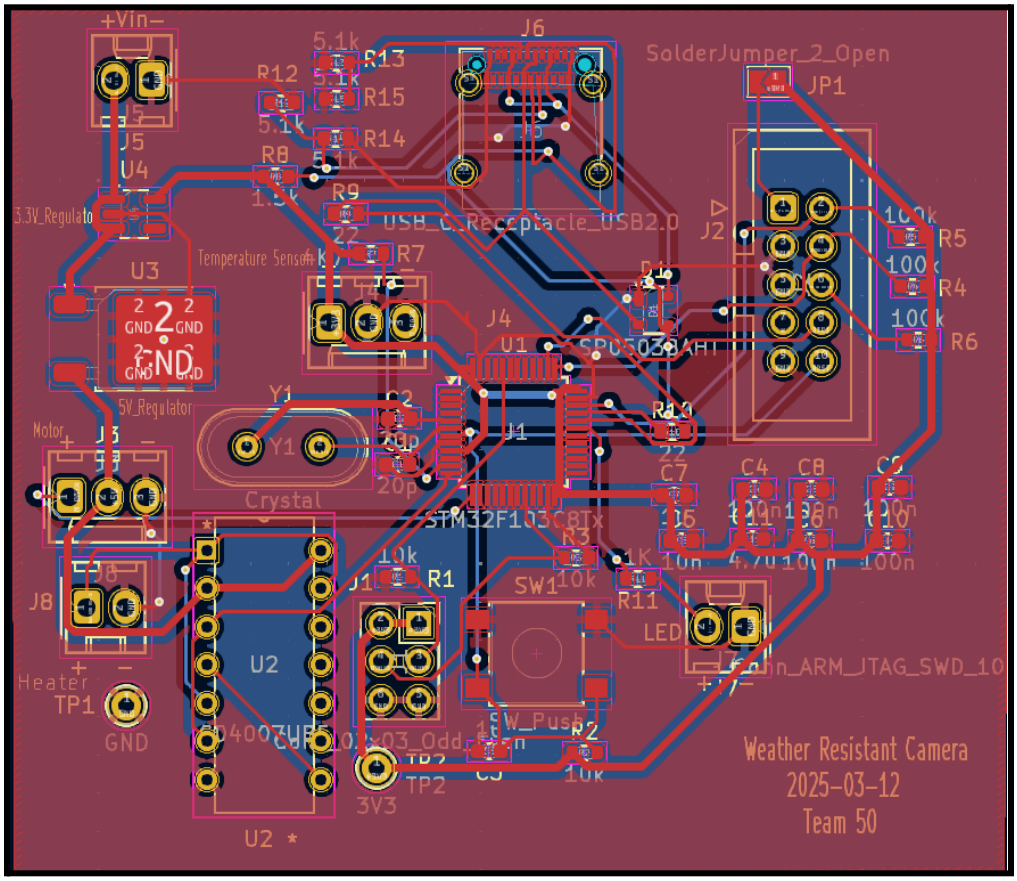

Figure 6: PCB Design

B.2.3 Physical Design

Figure 7: Physical Design (Front)

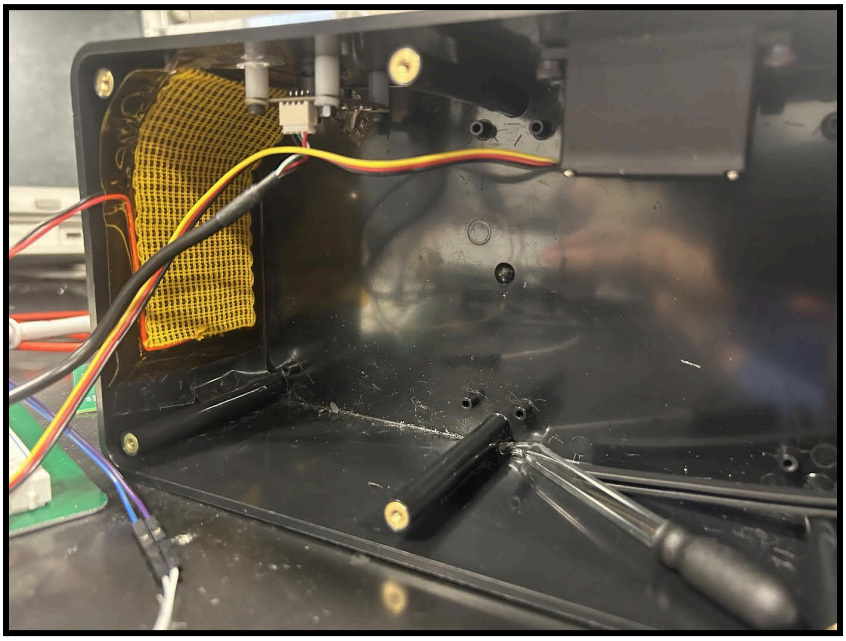

Figure 8: Physical Design (Inside)

Appendix C Costs & Schedule

C.1 Costs

Description	Manufacturer	Part #	Quantity	Cost
12 V 2400 mAh AA NI-MH Battery Pack with Standard Tamiya Connector	CBB	28RFLNK	1	$0.17
USB CAMERA FOR RASPBERRY PI	DFRobot	FIT0701	1	$9.90
WATERPROOF DIGITAL TEMPE	DFRobot	DFR0198	1	$6.90
IC REG LINEAR 3.3 V 600 MA SOT-25	Diodes Incorporated	AP2112K-3.3TRG1	1	$0.56
IC REG LINEAR 5 V 1A TO252	Rohm Semiconductor	BD50FC0FP-E2	1	$1.77
IC MCU 32BIT 64KB FLASH 48LQFP	STMicroelectronics	STM32F103C8T6	1	$6.01
NUCLEO-64 STM32F401RE EVAL BRD	STMicroelectronics	NUCLEO-F401RE	1	$13.82
HS-318 Servo-Stock Rotation	ServoCity	HS-318	1	$18.78
CONN RCP USB2.0 C 6POS SMD RA	Molex	2171750001	1	$0.75
HEATING PAD 5VDC 750MA	SparkFun Electronics	COM-11288	1	$4.50
JUMPER WIRE M/M 6" 20PCS	SparkFun Electronics	PRT-12795	1	$2.10
MOSFET-IC DUAL COMPL PAIR	Texas Instruments	CD4007UBE	2	$0.65
LED RED (5MM)	Broadcom Limited	HLMP-3301	1	$0.39
RES 100K OHM 1% 1/4W 0603	YAGEO	RC1206FR-07100KL	3	$0.10
RES 22 OHM 1% 1/4W 0603	YAGEO	RC1206FR-0722RL	2	$0.10
RES 5.1K OHM 1% 1/10W 0603	YAGEO	RC0603FR-105K1L	2	$0.10
RES 1.5K OHM 1% 1/4W 0603	YAGEO	RC1206FR-131K5L	1	$0.10
RES 10K OHM 1% 1/4W 0603	YAGEO	RC1206FR-1010KL	3	$0.10
TVS DIODE 5.5VWM SOT1434	Littelfuse Inc.	SP0503BAHTG	1	$0.70
CAP CER 0.1UF 50 V Z5U RADIAL	Vishay Beyschlag	1C20Z5U104M050B	5	$0.60
CAP CER 4.7UF 50 V X5R 1206	Murata Electronics	GRM319R61H475KA12D	1	$0.24
CAP CER 1UF 25 V X7R 0603	Samsung	CL10B105KA8NNNC	2	$0.06
CAP CER 20PF 250 V 0603	KYOCERA AVX	600S200FT250XT4K	2	$1.85
CAP CER 10000PF 0402 (10nF)	Murata Electronics	GRM155R71C103KA01D	1	$0.08
CRYSTAL 8.0000MHZ 20PF TH	ECS Inc.	ECS-080-20-4X-DU	1	$0.54
6" M/M Jumper Wires ONE WIRE price	SparkFun Electronics	PRT-12795	2	$0.17

Description	Manufacturer	Part #	Quantity	Cost
CONN HEADER VERT 6POS 2.54MM	Adam Tech	PH2-06-UA	1	$0.10
Machine Shop Labor Hours	*estimated*	*estimated*	10	$40/hr
				$476.87

Table 17: Itemized list of Components and Costs

C.2 Schedule

Week	Task(s)	Person
February 17th - February 23rd	· Finalize brainstorming project ideas · Solidify/Purpose final project idea	Adam
		Deyvik
		Jacob
February 24th - March 2nd	· Begin working on first PCB design · Order first round of parts needed for PCB	Adam
	· Research/test various models for raindrop detection	Deyvik
	· Begin working on first PCB design	Jacob
March 3rd - March 9th	· Work on Design Document · Work with temperature sensor to get correct readings	Adam
	· Work on Design Document · Finalize microcontroller code for breadboard demo · Finalize computer code for raindrop detection	Deyvik
	· Work on Design Document · Work with Servo Motor to generate proper PWM	Jacob
March 10th - March 16th	· Finalize first PCB design and place order · Prepare parts for the breadboard demo	Adam
		Deyvik
		Jacob
March 17th - March 23rd	Spring Break	
March 24th - March 30th	· Test PCB and revise design · Order second round of parts needed for PCB	Adam
	· Finish OpenCV code	Deyvik
	· Solder first Round PCB	Jacob

Week	Task(s)	Person
March 31st - April 6th	· Individual Progress Reports · Continue to revise any code or PCB design as needed · Place order for final PCB	Adam Deyvik Jacob
April 7th - April 13th	· Continue to revise any code or PCB design as needed	Adam Deyvik Jacob
April 14th - April 20th	· Prepare for mock/final demo	Adam Deyvik Jacob
April 21st - April 27th	· Mock Demo	
April 28th - May 4th	· Final Demo	

Table 18: Schedule for Project Progression